Simple Synthesis of 3D Ground-Moss-Shaped MnO@N-C Composite as Superior Anode Material for Lithium-Ion Batteries

Yanjun Zhai [1], Longhui Gai [1], Yingjian Gao [1], Ziwei Tong [2], Wenlin Wang [1], Huimei Cao [1], Suyuan Zeng [1], Konggang Qu [1], Gang Tian [3], Nana Wang [4] and Zhongchao Bai [5,*]

[1] Shandong Provincial Key Laboratory/Collaborative Innovation Center of Chemical Energy Storage and Novel Cell Technology, School of Chemistry and Chemical Engineering, Liaocheng University, Liaocheng 252059, China; zhaiyanjun@lcu.edu.cn (Y.Z.); glh35566@outlook.com (L.G.); gaoyingjian0396@163.com (Y.G.); 17568922686@163.com (W.W.); chm2728762036@163.com (H.C.); drzengsy@163.com (S.Z.); qukonggang@lcu.edu.cn (K.Q.)

[2] School of Chemical Engineering, the University of New South Wales Sydney, Kensington, NSW 2052, Australia; ziwei.tong@unswalumni.com

[3] Shandong Taiyi New Energy Co., Ltd., Liaocheng 252000, China; 18863588007@139.com

[4] Institute for Superconducting and Electronic Materials, University of Wollongong Innovation Campus, Wollongong, NSW 2500, Australia; nanaw@uow.edu.au

[5] Institute of Energy Materials Science, University of Shanghai for Science and Technology, Shanghai 200093, China

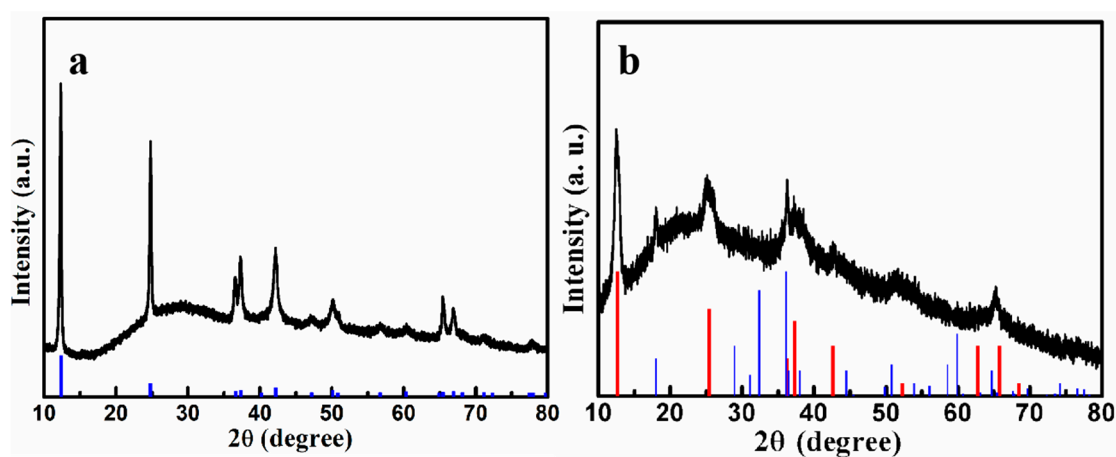* Correspondence: baizhongchao@tyut.edu.cn

Figure S1. XRD patterns for the precursors of (a) after hydrothermal reaction and (b) after coprecipitation at room temperature.
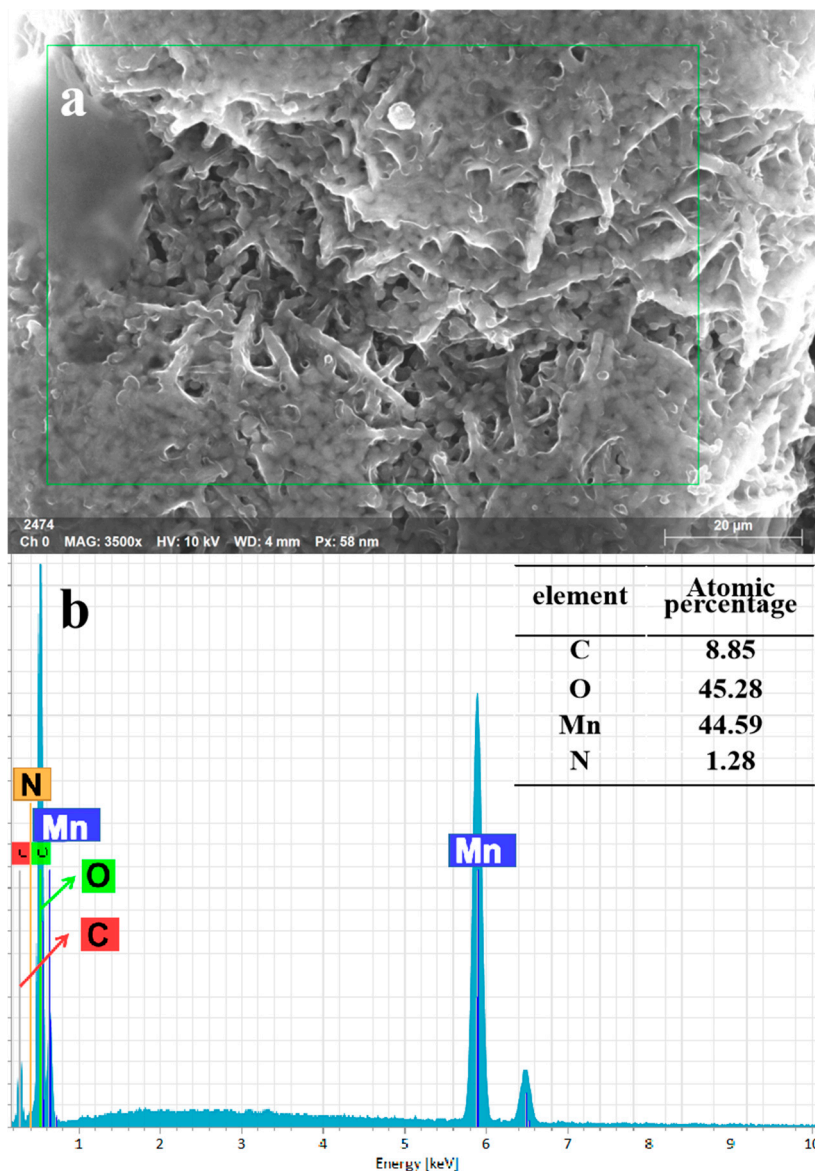
element	Atomic percentage
C	8.85
O	45.28
Mn	44.59
N	1.28

Figure S2. (a, b) EDX spectrum from SEM image of MnO@N-C. (Table inset i is the chemical composition of MnO@N-C.)
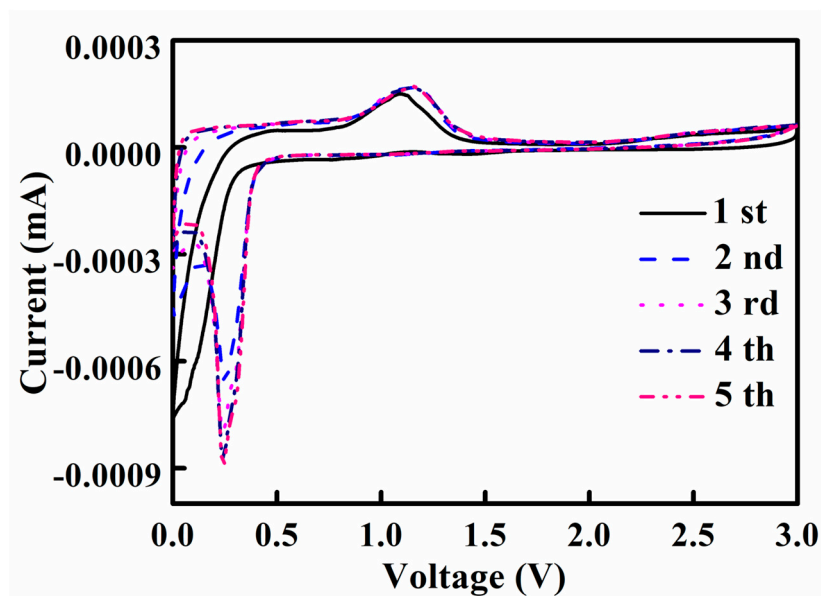
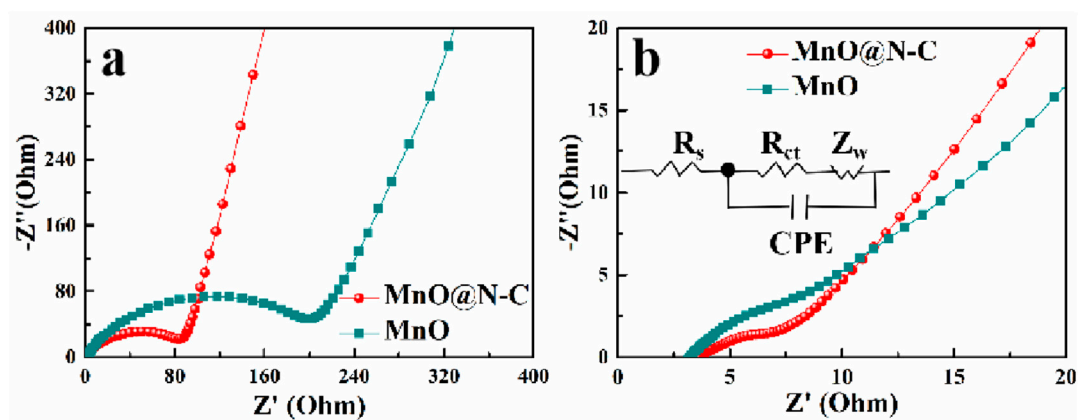**Figure S3.** CV curves of MnO electrode at 0.1 mV s^{-1}.

Figure S4. Nyquist plots of the MnO@N-C and MnO electrodes (a) before cycling, (b) after 50 cycles at 1 A g^{-1}. Insets is the corresponding equivalent circuit used.
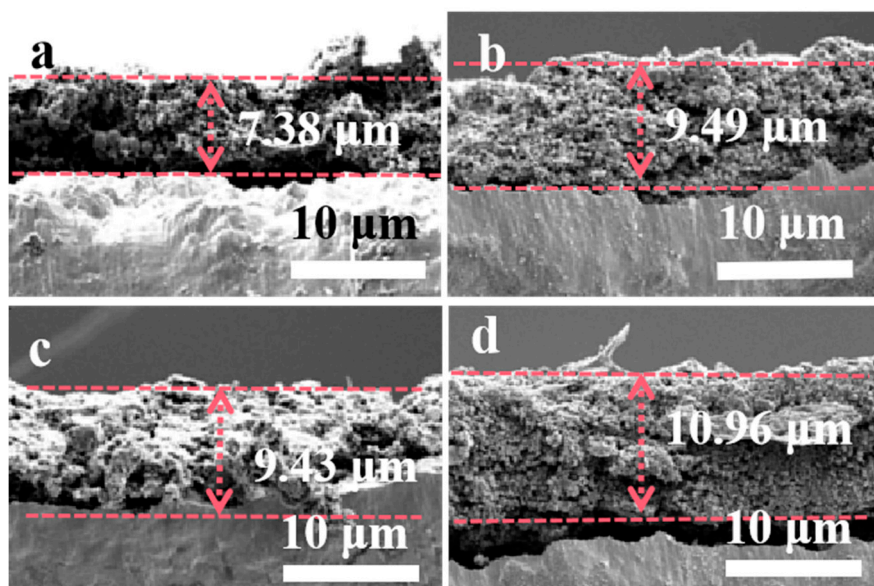
Figure S5. (a) SEM cross section of anode of Cu substrate before and after 50 cycles at 1 A g^{-1}: (a, c) MnO; (b, d) MnO@N-C.

Table S1. Peak Cent, FWHM, crystallite sizes and d-spacing are obtained from XRD data.

Sample	Peak Cent	FWHM	Crystallite Size D (nm)	Average D (nm)	d -spacing (nm)
MnO	34.88233	0.16957	49.50411188	44.2	0.269281183
	40.50755	0.18159	46.41599663		0.237087855
	73.74196	0.16695	52.38827141		0.180295563
MnO@N-C	34.9625	0.12551	66.88601072	66.7	0.268742063
	40.58301	0.12678	66.48664613		0.236723122
	58.71275	0.12826	66.874276		0.180206658

Table S2. Rs and Rct based on the EIS fitting outcomes of MnO@N-C and MnO.

	MnO@N-C	MnO
Rs (Fitted values)	2.13	2.18
Rct (Fitted values)	75.65	180.00
Rs (Fitted values) after 50 cycles	3.77	3.08
Rct (Fitted values) after 50 cycle	9.09	14.81

Table S3. Comparison of lithium storage performance between MnO@N-C and other reported MnO and N-doped C based electrodes.

Materials	Preparation Method	Organic Reagent	ICE (%)	Current density (A g^{-1})	Capacity (mAh g^{-1}) after cycles	Ref.
3D ground moss shaped MnO@N-C	hydrothermal-coprecipitation-annealing (600 °C)	Tris-buffer (0.01 M, pH=8.5),PDA	72.1	0.1	808,80	This work
			73.2	1.0	563, 300	
3D MnO@N-doped C	Vacuum freeze drying-calcination (700 °C)	glucose (C$_6$H$_{12}$O$_6$), urea (CH$_4$N$_2$O)	69	0.1	1037.0, 100	1
				5.0	760.9, 500	
MnO/N-doped carbon nanosheets	salt-templated-calcination (800 °C)	dicyandiamide (C$_2$H$_4$N$_4$)		1	497, 100	2
			63	0.1	719，10	
MnO@NC composites	coprecipitation-calcination (400 °C)	cpolyacrylonitrile (PAN) , dimethylformamide (DMF)		0.1	998, 100	3
				0.5	629, 500	
MnO@N-C microcube	coprecipitation-annealing (700 °C)	Tris-buffer (0.01 M, pH=8.5) ,PDA		0.1	1009, 10	4
				5.0	576, 3500	
MnO@N-C S-M	coprecipitation-annealing (900 °C)	glucose (C$_6$H$_{12}$O$_6$), urea (CH$_4$N$_2$O)	53.5	0.2	917, 190	5
				1.0	650, 550	
NC/Co-MnO composites	hydrothermal-coprecipitation-annealing (550 °C)	2-Methylimidazole Polyvinylpyrrolidone (PVP)		0.2	~1100, 120	6
1D MnO@N-doped C nanotubes	hydrothermal-coprecipitation-annealing (500 °C)	Tris-buffer (0.01 M, pH=8.5),PDA	74.2	0.1	980,10	7

1. He, C.; Li, J.; Zhao, X.; Peng, X.; Lin, X.; Ke, Y.; Xiao, X.; Zuo, X.; Nan, J. In situ anchoring of MnO nanoparticles into three-dimensional nitrogen-doped porous carbon framework as a stable anode for high-performance lithium storage. *Applied Surface Science* **2023**, *614*, 156217.

2. Liu, J.; You, F.; He, B.; Wu, Y.; Wang, D.; Zhou, W.; Qian, C.; Yang, G.; Liu, G.; Wang, H. Directing the architecture of surface-clean Cu$_2$O for CO electroreduction. *Journal of the American Chemical Society* **2022,** *144* (27), 12410-12420.

3. Hong, Y.; Hu, Q.; Dong, H.; Li, J.; Tang, Z.; Wang, X.; Ouyang, J.; Liu, T. J. S. M., N-doped carbon coated porous hierarchical MnO microspheres as superior additive-free anode materials for lithium-ion batteries. *Scripta Materialia* **2022,** *211*, 114495.

4. Lin, J.; Yu, L.; Sun, Q.; Wang, F.; Cheng, Y.; Wang, S.; Zhang, X. Multiporous core-shell structured MnO@N-Doped carbon towards high-performance lithium-ion batteries. *International Journal of Hydrogen Energy* **2020,** *45* (3), 1837-1845.

5. Huang, S.; Li, H.; Xu, G.; Liu, X.; Zhang, Q.; Yang, L.; Cao, J.; Wei, X. Porous N-doped carbon sheets wrapped MnO in 3D carbon networks as high-performance anode for Li-ion batteries. *Electrochimica Acta* **2020,** *342*, 136115.

6. Gong, Y.; Sun, L.; Si, H.; Zhang, Y.; Shi, Y.; Wu, L.; Gu, J.; Zhang, Y. MnO nanorods coated by Co-decorated N-doped carbon as anodes for high performance lithium ion batteries. *Applied Surface Science* **2020,** *504*, 144479.

7. Gan, Q.; He, H.; Zhao, K.; He, Z.; Liu, S. Preparation of N-doped porous carbon coated MnO nanospheres through solvent-free in-situ growth of ZIF-8 on $ZnMn_2O_4$ for high-performance lithium-ion battery anodes. *Electrochimica Acta* **2018,** *266*, 254-262.